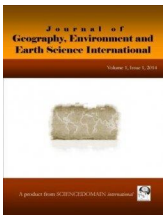

Journal of Geography, Environment and Earth Science International
10(1): 1-22, 2017; Article no.JGEESI.30741
ISSN: 2454-7352

SCIENCEDOMAIN *international*
www.sciencedomain.org

Geological Interpretation of the High Resolution Aeromagnetic Data over Okigwe-Udi Area, Anambra Basin, Nigeria, Using 3-D Euler Deconvolution and 2-D Spectral Inversion Methods

R. A. Onyewuchi[1*] and S. A. Ugwu[2]

[1]Department of Geology, University of Port Harcourt, Rivers State, Nigeria.

Authors' contributions

This work was carried out in collaboration between both authors. Author RAO performed the statistical analysis, wrote the protocol and the first draft of the manuscript. Author SAU designed the study. Authors RAO and SAU managed the analyses of the study and managed the literature searches. Both authors read and approved the final manuscript.

Article Information

DOI: 10.9734/JGEESI/2017/30741
Editor(s):
(1) Anthony R. Lupo, Department of Soil, Environmental, and Atmospheric Science, University of Missouri, Columbia, USA.
Reviewers:
(1) Efosa Udinmwen, University of Calabar, Nigeria.
(2) Okpoli Cyril Chibueze, Adekunle Ajasin University, Ondo State, Nigeria.
Complete Peer review History: http://www.sciencedomain.org/review-history/18815

Original Research Article

Received 28th November 2016
Accepted 28th March 2017
Published 26th April 2017

ABSTRACT

Geological interpretation of the high resolution aeromagnetic data over Okigwe-Udi area Southeastern Nigeria, was carried out using 2-D spectral inversion and 3-D Standard Euler deconvolution methods. The objectives of the study are to delineate subsurface geological features, estimate the depth to anomalous magnetic bodies, map basement topography and infer the contribution of the interpreted features to the mineral and hydrocarbon potentials of the study area. The acquired magnetic data was enhanced to separate residual features relative to the strong regional gradients and other more intense magnetic anomalies due to basement features and igneous intrusives. The spectral inversion computational method used in the study transformed the spatial data into the frequency domain and provided a relationship between the radially averaged power spectrum of the magnetic anomalies and the depths to the respective sources. Similarly, the

**Corresponding author: E-mail: regonye28@yahoo.co.uk;*

3-D Standard Euler Deconvolution method examined the shape of the magnetic field within a window and calculated the 3-D source locations based on magnetic structural indices (SI). Results of the 2-D spectral analysis revealed a two layer depth model with the shallower magnetic source depth varying from 0.223 to 1.048 km (d_1) with an average depth of 0.641 km while the deeper magnetic source bodies (d_2) depth varies from 2.659 km to 3.748 km with an average depth of 3.088 km. Linear features delineated from the study revealed a predominance of NE-SW trending structures within the study area. Structural interpretation using 3-D Euler deconvolution with structural index values of 0 to 3, revealed three dominant structural models which include spheres, horizontal pipes/cylinders and sills/dykes. In addition, magnetic depth estimates made from 3-D Standard Euler deconvolution revealed a depth range of 0 to 3.0 km. Despite the fairly appreciable sedimentary thickness, the hydrocarbon potential of the study area is low owing to the presence of pyroclastics in the area which is a strong indication of previous igneous activities.

Keywords: Basement depth; geological interpretation; aeromagnetic; Anambra basin; spectral inversion; Euler deconvolution.

1. INTRODUCTION

Geological interpretation among other things involves detailed surface and subsurface mapping of the lithology, delineation of associated structural features and the interpretation of basement tectonics and geodynamical processes within the study area. The use of airborne magnetic data in the delineation of structural discontinuities and determination of depth to anomalous bodies has witnessed an overwhelming interest within the past three decades. Similarly, this period has seen the application of aeromagnetic surveys from interpretation of solely basement structures to detailed examination of structures and lithology [1]. Airborne magnetic survey has proved essential in displaying the spatial distribution and relative abundance of magnetic and non-magnetic minerals in the upper levels of the crust which can help in the visualization of the geology and geological structures of the upper crust of the earth [1]. Basement structures and depths therefore can be delineated and mapped accurately using magnetic data. If the magnetic units in the basement occur at the basement surface, then depth determinations for these anomalous bodies will map the basin floor topography, morphology and structure with a relatively high accuracy [2]. In many sedimentary basins, magnetic anomalies arise from secondary mineralization along fault planes, which are often revealed on aeromagnetic maps as surface linear features. Most mineral deposits are generally related to some type of deformation of the lithosphere and most theories of ore formation and concentration embodies tectonic or deformational concepts [3]. Definition of various basin and sub-basin geometries, structures and geodynamics can enable the mapping of the regional hydrocarbon and mineral fetch areas.

Trends in magnetic features most often have semblance to the trend of the overlying sediment as sedimentary structures are to a large extent are controlled by basement tectonics. The determination of depth to anomalous basement helps in the location of mineralized zones as well as the evaluation of the hydrocarbon prospectivity of the region. The magnetic anomaly signature characteristics are results of one or more physical parameters such as the configuration of the anomalous zone, magnetic susceptibility contrast as well as the depth to the anomalous body. The broad magnetic closures seen on the total magnetic intensity anomaly maps are often due to changes in the rock composition within the basement. Depth to basement, faults in the basement surface, and the relief of the basement surface have direct relevance to the depositional and structural history of the study area. These geological structures are often overlain by sediments whose depositional isopachs and/ or structure reflect the underlying basement structure [1]. Thus, through the study of the magnetic basement, information can be provided on the morphology of the sedimentary basin and its structure. Therefore, source depth or location of anomalies can be interpreted from contoured aeromagnetic maps.

Magnetic depth methods are generally based on the transformation of the potential field anomalies into special functions that form gradient peaks and ridges over the sources. The spectral depth method is based on the principle that a magnetic field measured at the surface can therefore be considered to be an integral of magnetic

signatures from all depths. The application of 2-D spectral inversion to the interpretation of potential field data is one method that has been used to determine the basement depth, and is now sufficiently well-established [4]. Several authors have used spectral inversion techniques in the determination of sedimentary thickness of basins elsewhere [5-10]. Similarly, Euler deconvolution method examines the shape of the magnetic field within a window and calculate the three-dimensional source locations based on the various magnetic structural index values (MSI).The structural index describes the rate at which the potential field decays based on source geometry and is specified based on expected target geometry.

The knowledge of sedimentary overburden thickness is vital especially for the exploitation of ore minerals and construction materials. Depth to anomalous magnetic source interpretation provides clue to the sedimentary basin architecture for hydrocarbon exploration as well as the presence of minerals. Geologically, the established presence of oil shows, igneous intrusive bodies and pyroclastics in some parts of the study area has generated a lot of discourse within the geological community. The geological interpretation of the high resolution aeromagnetic data of the study area will further provide additional clarification of the basement depth, structural and tectonic history and mineral and hydrocarbon potential assessment of the study area This paper therefore presents the detailed interpretation of the airborne magnetic data over Udi-Okigwe area of the Anambra basin with the objectives of mapping the geological features associated with the study area as well as the estimation of depth to anomalous magnetic bodies by incorporating 3-D Euler deconvolution and 2-D spectral methods.

1.1 Geology of Study Area

The study area occupies part of the Anambra basin, southern Benue Trough. Its southern boundary coincides with the northern boundary of the Niger delta basin. The basin extends northward beyond the lower Benue River. The southern part of the Anambra basin is a part of the scarp lands of southeastern Nigeria. The north- south trending escarpment forms the major watershed between the lower Niger drainage system to the west, the Cross and Imo River's drainage systems to the east. The escarpment is an asymmetrical ridge stretching in a sigmoid curve for over 500km from Idah on the Niger River to Arochukwu in Abia State [11]. The structural setting and general geology of the Anambra Basin have been documented by various workers [14,15,23]. The Anambra Basin is located in the southwestern end of the Benue Trough of Nigeria. It is delimited by latitudes 5° 30' to 7° 00'N and longitudes 7° 00' to 8° 00'E (Fig. 1).

The tectonic framework of the continental margin along the west coast of equatorial Africa is controlled by cretaceous fracture zones expressed as trenches and ridges in the deep Atlantic. The evolution of the Southern Nigeria sedimentary basin originally developed during the breakup of the South American and African plates in the late Jurassic [12,13]. The Cretaceous Anambra Basin, Southeastern Nigeria consists of rhythmic clastic sequences of sandstones, shales, siltstones, mudstones, sandy shales with interbedded coal seams. It covers an area of about 40,000 km^2 [11]. The stratigraphic history of the region is characterized by three sedimentary phases [14,15,11] during which the axis of the sedimentary basin shifted. These three phases were: (i) the Abakaliki-Benue Phase (Aptian-Santonian), (ii) the Anambra-Benin phase (Campanian-Mid Eocene), and (iii) the Niger Delta phase (late Eocene- Pliocene). The first sedimentary phase led to the deposition of over 3000 metres of rocks comprising: the Asu River Group, the Ezeaku and Awgu Formations, in the Abakaliki-Benue Basin, the Benue Valley and the Calabar Flank. This phase produced two principal sets of faults, trending NE-SW and NW-SE. The NE-SW set of faults bound the Benue Trough; while the NW-SE sets defined the Calabar Flank. The second resulted from the Santonian tectonic episode of Abakaliki region and dislocation of the depocenter into the Anambra Platform and Afikpo region. The resulting succession is made up of: The Nkporo Group, Mamu Formation, Ajali Sandstone, Nsukka Formation, Imo Formation and Ameki Group. The Santonian deformation was characterized by compressive folding, generally along a NE-SW direction, parallel to the trough margin. The folding episode that took place during the Santonian strongly affected the development of the Abakaliki Anticlinorium. The predominantly compressional nature of the folds that developed during this period is revealed by their asymmetry and the reversed faults associated with them. [16], in a detailed report of geology of Abakaliki suggests that the compression responsible for the large scale folding and cleavage was directed

N155^{o} E. The magmatism that occurred resulted in the injection of numerous intrusive bodies into the shale of the Eze-aku and Asu River Group. The final phase witnessed the formation of the petroliferous Niger Delta which started during the Eocene as a result of a major earth movement that structurally inverted the Abakaliki region and displaced the depositional axis further to the south of the Anambra Basin [14].

The study area is underlain by sedimentary facies which include: the Asu River Group, the Eze-aku Formation, The Awgu Shale Group, Nkporo Shale, Mamu Formation, Ajali Formation, Imo Shale, Ameki Formation, Ogwashi-Asaba Formation and Benin Formation. The Asu River Group (Albian-Cenomanian) consists of alternating sequence of shales and siltstones with occurrences of sandstone having its maximum thickness as 1500 m. It represents the first and oldest cycle of shallow marine to brackish water sediments deposited on the basement complex. There has been reported presence of Cenomanian sediments and Santonian intrusives of dykes and sills extrusives. The Eze-aku Formation (Turonian-coniacian) comprises flaggy calcareous shale with thin sandy or shaley limestone and calcareous siltstone. Eze-aku Formation overlies the Asu River Group with the formation deposited as a result of renewed transgression in the second depositional cycle of the Benue Trough. The thickness of the Eze-aku Formation is highly variable and may get to a thickness of 1200 m [17,18]. The Awgu Shale (Coniacian) consists of shale with thin limestone bands and lenticular sand bodies. It is deposited in a marine environment. The Nkporo Shale Formation (late Campanian – Maastrichtian) was deposited in various environmental settings including shallow open marine paralic and continental regimes [19]. It consists of dark grey, fissile shale, brown silty and sandy shale, mudstone and fine-grained sandstone. Mamu Formation (Maastrichtian) comprises tidal estuarine facies dominated by poorly consolidated carbonaceous sandstones, siltstones and mudrock with coal seams [19]. The Ajali Formation consists of mainly fluvial to marginal marine facies comprising unconsolidated to poorly cemented, coarse to fine grained sandstones, siltstones and carbonaceous mudrock which are characterized by a lateritic surface [19]. The Ajali Formation is overlain by the Paleocene Imo Shale Formation which is characterized by well laminated blue and dark grey clayey shales with occasional bands of calcareous sandstone, marls, and limestone. [20] Identified two depositional sequences in the Imo Shale with each bearing a striking similarity to estuarine cycles. The shales are very compacted, unjointed and impervious. Large ventricular sands often occur in places. Gravelly and silty sandstones units of the Umuna and Ebenebe sandstones are also interbedded within this formation but these members have limited coverage. The Imo shale was deposited under marine conditions. Shallow marine clastics facies and deeper marine clastic facies can be recognized [15]. The Eocene to Oligocene aged Ameki Formation consists of medium to coarse-grained white sandstone, bluish calcareous silt, with mottled clays and thin limestone. Ameki Formation is characterized by lateral and vertical variations in lithology [21,22]. Its lateral equivalent is the Nanka Sands. The lithologic units of the Ameki Formation are divided into two general groups [23,22]: The upper grey-green sandstones and sandy clay; and a lower unit with fine to coarse sandstones and intercalations of calcareous shales and thin shelly limestone. The Ogwashi-Asaba Formation (Oligocene) consists generally of an alternation of seams of lignite with clays. This Formation represents the Nigerian lignite formation [23]. The Benin Formation is the youngest formation (Miocene to Recent) in the study area. It made contact with the Ameki and Ogwashi-Asaba Formations and dips south westward. The Benin Formation consists mainly of sandstone and clays. The Benin Formation is partly marine and partly continental. The Benin Formation consists of thick friable sands with lintel intercalations of clay beds and lenses. Its thickness ranges from 200 to 2000 metres within certain areas across the region.

The abundance of pyroclastics and intrusives which are associated with explosive eruption of lava and magmatic processes respectively; have been observed widely in most part of the study area especially around Lokpanta and Lokpaukwu. These pyroclastics are interpreted as being subaerial falls of submarine explosions during the upper Albian [24]. Elsewhere pyroclastics occur in places such as: Ngbo and Abakaliki Juju hill within the Abakaliki Anticlinorium [25]. The deposition of pyroclastics in these places reflects the past igneous activities which must have taken place in the study area.

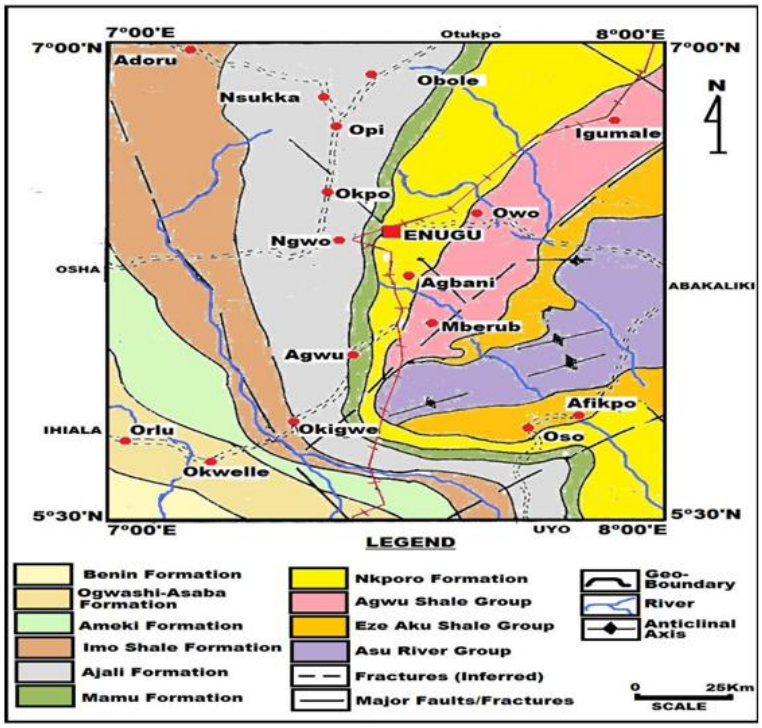

Fig. 1. Geological map of the study area

2. MATERIALS AND METHODS

Aeromagnetic sheets 301 (Udi) and 312 (Okigwe) were used for this study. Airborne geophysical data acquired from 2007 to 2008 by FUGRO Nig. Ltd in collaboration with the Nigerian Geological Survey Agency (NGSA) was processed for this study. Flight line direction was NNW-SSE at station spacing of 0.5 km with flight line spacing of 0.5 km at an altitude of about 80 m terrain clearance. Tie lines were flown in an ENE-WSW direction. Regional correction of the magnetic data was based on the IGRF (epoch date of 1st January, 2000). For this study, aeromagnetic sheets 301 and 312 were used which covered the area within latitudes 5°30' - 6°30'N and longitudes 7° 00'- 7° 30'E. These maps are published on a scale of 1:100,000. The regional gradients were removed by fitting a plane surface to the data by multi- regression least squares analysis.

The aeromagnetic map came in digital form and of higher quality due to improvement in technology and powerful error correcting software that was used in the processing. The nature of filtering applied to the aeromagnetic data in this study was chosen to eliminate certain wavelengths and to pass longer wavelengths. Analytical methods used include 2-D spectral inversion, trend surface analyses, upward continuation and 3-D Euler deconvolution. The main software used for the processing and enhancement of the aeromagnetic were: Geosoft Oasis Montaj (version 6HJ), U.S. Geological Survey.

The residual anomalies in the original aeromagnetic field map were modeled in terms of intrusions using non-linear optimization techniques built in MATLAB 7.0 software. The method is targeted at minimizing a non-linear objective function which represents the difference between the observed and calculated fields through an iterative change of the non-linear parameters (location, thickness and depth) by non-linear optimization while at the same time obtaining optimum values for the linear parameters (magnetization components, quadratic regional and composite magnetization angle) by least-square analysis. Graphical methods (Peter's, slope method, Hannel and Tiburg methods) were used in calculating depth estimates to the anomalous bodies (Figs. 6a and 6b). The estimated depths and linear parameters are presented in Table 2. Potential-Field geophysical software (Version 2.2), Surfer 12 and Matlab 7.5.

2-D spectral inversion allows for estimation of the depth of an ensemble of magnetized blocks of varying depth, width, thickness and magnetization was also carried out in this study. These depths were established from the slope of the log- power spectrum at the lower end of the total wave number or spatial frequency band. The method allows an estimate of the depth of an ensemble of magnetized blocks of varying depth, width, thickness and magnetization. Most of the approaches used involve Fourier transformation of the digitized aeromagnetic data to compute the energy (or amplitude) spectrum. This is plotted on a logarithmic scale against frequency. The slopes of the segments yield estimates of average depths to magnetic or gravity sources of anomalies. Given a residual magnetic anomaly map of dimensions l x l, digitized at equal intervals, the residual total intensity anomaly values can be expressed in terms of a double Fourier series expression given as:

$$T(x, y) = \sum_{n=1}^{N} \sum_{m=1}^{M} P_m^n \text{Cos}\{(\frac{2\pi}{l})(nx + my)\} + Q_m^n Sin\{(\frac{2\pi}{l})(nx - my)\} \quad (1)$$

where, l = dimensions of the block, and is the Fourier amplitude and N and M are the number of grid points along the x and y directions respectively. Similarly, using the complex form, the two dimensional Fourier transform pair may be written as:

$$G(u,v) = \iint_{-\infty}^{\infty} g(x,y)\, e^{-j(u_x|+v_y)}\, dx\, dy \quad (2)$$

and

$$g(x,y) = \iint_{-\infty}^{\infty} G(u,v) e^{j(u_x+|v_y)}\, du\, dv \quad (3)$$

Where, u and v are the angular frequencies in the x and y directions respectively.

The use of this method involved some practical problems, most of which are inherent in the application of the Discrete Fourier Transform (DFT). These include the problems of aliasing, truncation effect or Gibb's phenomenon and the problems associated with even and odd symmetries of the real and imaginary parts of the Fourier transform. However, some of the associated problems were addressed by the software used in the analysis.

Similarly, standard 3-D Euler deconvolution produces maps that show the locations and depth of geological sources. Euler deconvolution is commonly employed in magnetic interpretation because it requires only a little prior knowledge about the magnetic source geometry, and more so, it requires no information about the magnetization vector [26,27]. The method examines the shape of the magnetic field within a window and calculate three-dimensional source locations based on a structural index (SI). The structural index describes the rate the field decays based on source geometry and is specified based on expected target geometry in standard Euler deconvolution. For example, it is commonly agreed in the potential field community that the SI should be between 0 and 0.5 in order to find basement depths. Source locations and depth estimation may be marred by noise. The Standard 3-D Euler method is based on the fact that the potential field produced by many simple sources obeys Euler's homogeneity equation [10]. This equation relates the potential Field (magnetic) and its gradient components to the location of the sources, by the degree of homogeneity N, which can which can be interpreted as a structural index [26]. The method makes use of a structural index in addition to producing depth estimates. Simultaneous use of the depth estimates and structure indices have the potential to calculate depth and determine the geological structures such as: faults, magnetic contacts, dykes, sills, etc. The algorithm uses a least squares method to solve Euler's equation simultaneously for each grid position within a sub-grid (window). A square window of pre-defined dimensions (number of grid cells) is moved over the grid along each row. At each grid point, a system of equations is solved from which the four unknowns (x, y as location in the grid, z as depth estimation and the background value) and their uncertainties (standard deviation) are obtained for a given structural index. If a given component of the anomalous magnetic field ΔT (x; y; z) satisfies:

$$\Delta T(tx; ty; tz) = t^n \Delta T(x; y; z) \quad (4)$$

Where *n* is the degree of homogeneity, then by differentiating Eq. (4) with respect to *t*, it can be shown that:

$$x\frac{\delta \Delta T}{\delta x} + y\frac{\delta \Delta T}{\delta y} + z\frac{\delta \Delta T}{\delta z} = n\Delta T \quad (5)$$

Where, x, y,and z are the coordinates of field observation points and source is assumed to be at the origin. Equation 5 is Euler homogeneity equation [28,27,26]. The degree of homogeneity is source dependent and characterizes how fast the field decreases as a function of distance to the source.

The function ΔT (x; y; z) can have a general function form [26-29]:

$$\Delta T\,(x; y; z) = \frac{G}{r^N} \quad (6)$$

Where $r^2 = (x - x_0)^2 + (y - y_0)^2 + (z - z_0)^2$, N is a real number (1,2,3.) and G a constant (independent of x,y,z). Many simple point magnetic sources can be described by equation 6 above, with (x_0; y_0; z_0) the position of the source whose field F is measured.

Since the potential field is inversely proportional to the distance raised to some power, the degree of homogeneity is non-positive. The negative of the degree of homogeneity is defined as the structural index (SI) and will be denoted as N. Table 1 gives a summary of the structural indices (SI) for some known geologic models. The number of infinite dimensions describes the extension of the geologic model in space.

Table 1. Structural indices for simple magnetic models used for depth estimations by 3-D Euler Deconvolution

Geologic model	Number of infinite dimension	Magnetic structural index
Sphere	0	3
Horizontal cylinder	1(x-y)	2
Pipe	1(z)	2
Dyke	2 (z and x-y)	1
Sill	2 (x and y)	1
Contact	3 (x, y, z)	0

With appropriate choice of structural indices, 3-D Euler deconvolution will lead to clustering of solutions which can be interpreted geologically. A sill for example can be seen as a cluster of solutions around a curvature. A vertical pipe structure will show as a cluster of solutions around a specific point while an elongated dyke structure will be recognized as a linear trend of solutions.

3. RESULTS AND DISCUSSION

The aeromagnetic data of the study is presented as a total magnetic field intensity map (Fig. 2). The magnetic intensity values in the study ranges from 7740 to 8020 gammas, with an average of 7880 gammas. Magnetic anomalies of both short and long wavelengths represented by magnetic highs and lows were reveled on the total magnetic field intensity map of the study area (Fig. 2). Alternations of regions of high and low magnetic anomalous values were observed on the total field intensity map (Fig. 2) indicating high and low basement relief respectively. The high basement relief may be interpreted as the crest of folds of intrusive bodies, whereas the low basement relief may correspond to the trough or areas where the basement may have subsided. The total magnetic field intensity map (Fig. 2) of the study area also revealed prominent linear and curvilinear magnetic anomalies associated with sharp gradients as well as positive and negative closures. The linear features identified on the magnetic intensity map (Fig. 2) were interpreted using [30] criteria which include abrupt termination of linear highs and/or lows, abrupt changes in the linear gradients, linear contour patterns and any combination of the preceding criteria. The two major magnetic lineations seen on the map (Fig. 2) in the northern and central portions of the study area have continuous linear contour patterns, running across the entire map which strikes in the NE-SW direction. However, linear features striking in the E-W direction were observed in the east-central portion of the study area. There are abrupt termination of magnetic highs and lows in the southwestern portion of the study area which revealed possible presence of linear anomalies in those areas. Lineaments with NE-SW trend were observed at the boundary of the alternating high and low magnetic regions. These broad magnetic highs and lows are believed to be of regional extent. The observed broad low magnetic intensity in the lower central portion of the map suggests linear features of deep-seated tectonic origin within the area.

The observed alternate regions of high and low magnetic anomalies from the intensity map (Fig. 2) appear as a folded basement magnetic surface on the 3-D map (Fig. 3) [31] reported that several clusters of circular magnetic anomalous closures with different amplitudes may be interpreted to be lithological variations of mafic–ultramafic inclusions within granodioritic batholiths. The 3-D map revealed spiky surfaces around the central and southern portions of the study area which are suspected intrusive bodies probably originating from magmatic intrusion into the sedimentary rocks. These areas have been affected by magmatic processes of intrusive mechanism. The distribution of mafic and felsic rock forming minerals were correlated to clusters seen on the standard Euler deconvolution maps (contact) for the study area. The areas with high magnetic intensity values and spiky surfaces are believed to have been more tectonically active in the past than the rest of the study.

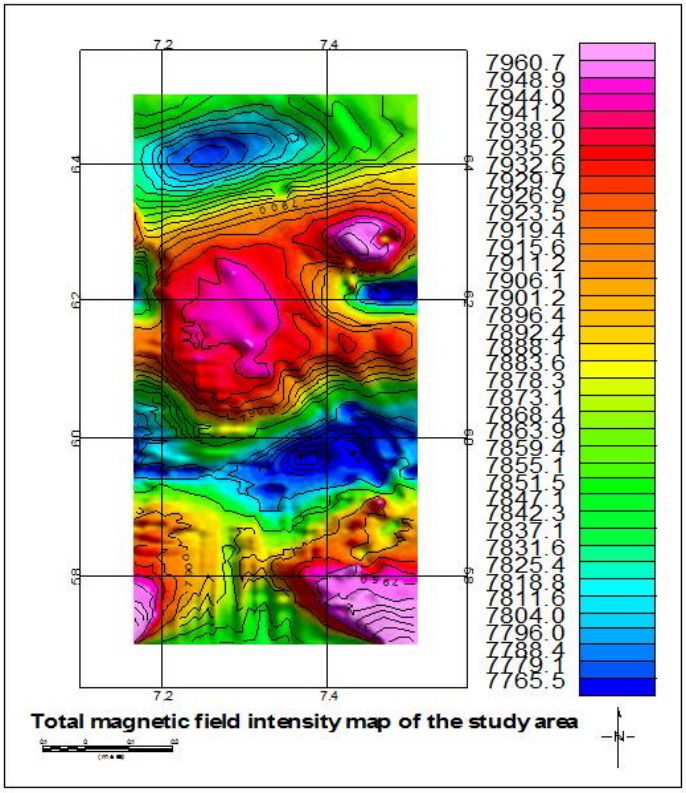

Fig. 2. Total magnetic field intensity contour map of the study area

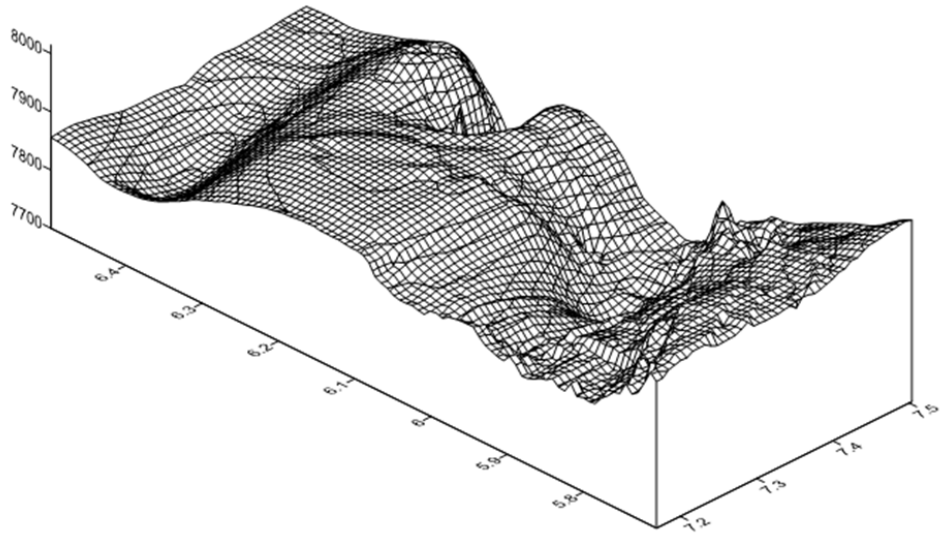

Fig. 3. Total Field of the aeromagnetic data presented as 3-D map showing the basement topography

Interpreted structural trends of the aeromagnetic maps (Figs 2-5) revealed trends in the directions of NE-SW, E-W and NW-SE. The first degree regional polynomial surface revealed a NE-SW trend and therefore defined the orientation/trend of the basin of the study area. This is in agreement with the earlier work by [32] on the Benue Trough. The interpreted NE-SW trend

from the first degree regional polynomial surface (Fig. 4) represents the main magnetic trend which reflects the old and deeper tectonic trends. Similarly, interpretation of the surface linear features from Landsat Enhanced Thematic Mapper Plus (Landsat-ETM+) data revealed several lineaments. Analysis of the trends of these surficial lineations using azimuth frequency diagrams generated from the plot of the strikes and frequencies of the sampled lineations revealed trends in the NE-SW, E-W and WNW-ESE directions (Figs. 6 and 7). Similarly, the dominant surface trend derived from the Landsat data showed a NE-SW trend. Generally, the regional field is often used to establish the major tectonic elements that affected the structural framework of the study area. The dominant NE-SW trend interpreted from the study area is in line with the results of earlier scholars [12,33,34].

The residual magnetic field of the study area revealed values ranging between -101.6 to 98.7 gammas (Fig. 5). The high magnetic relief interpreted on the total field map (Fig. 2) shows up as positive residual anomalies with values of 62.2 to 98.7 gammas. Similarly, the low magnetic relief areas appears as negative residual anomalies with values of -73.4 to -101.6 gammas. Negative residual anomaly values were also observed around the central, the northern and the southern fringes of the study area. Positive residual magnetic intensity were also interpreted around Enugu and Okigwe areas. Whereas positive residual magnetic values indicate high magnetization, negative values reflect low magnetization. This implies that there is an existence of shallow to near surface magnetized bodies in areas such as Enugu and Okigwe which have positive residual peaks.

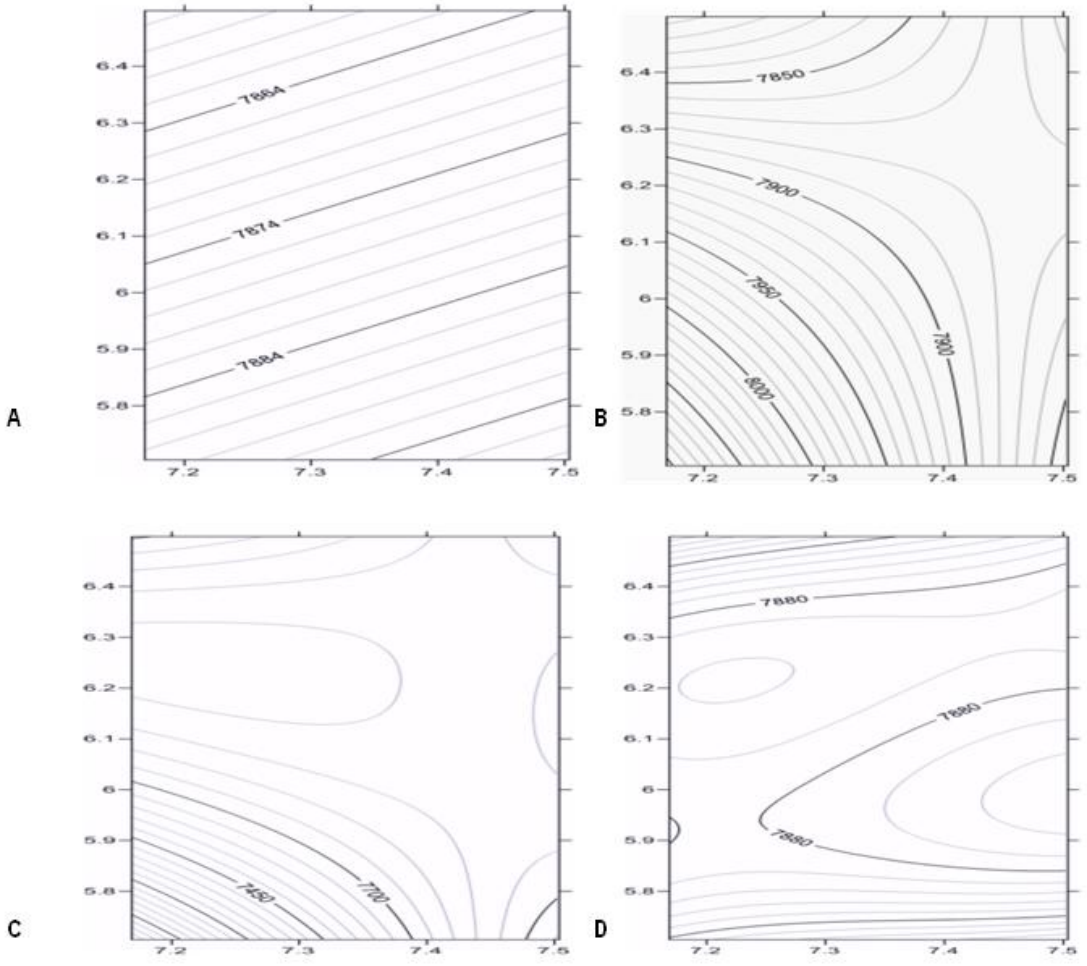

Fig. 4. First to fourth degree (polynomial) surfaces of the aeromagnetic data: (a) First degree (b) Second degree (c) Third degree (d) Fourth degree

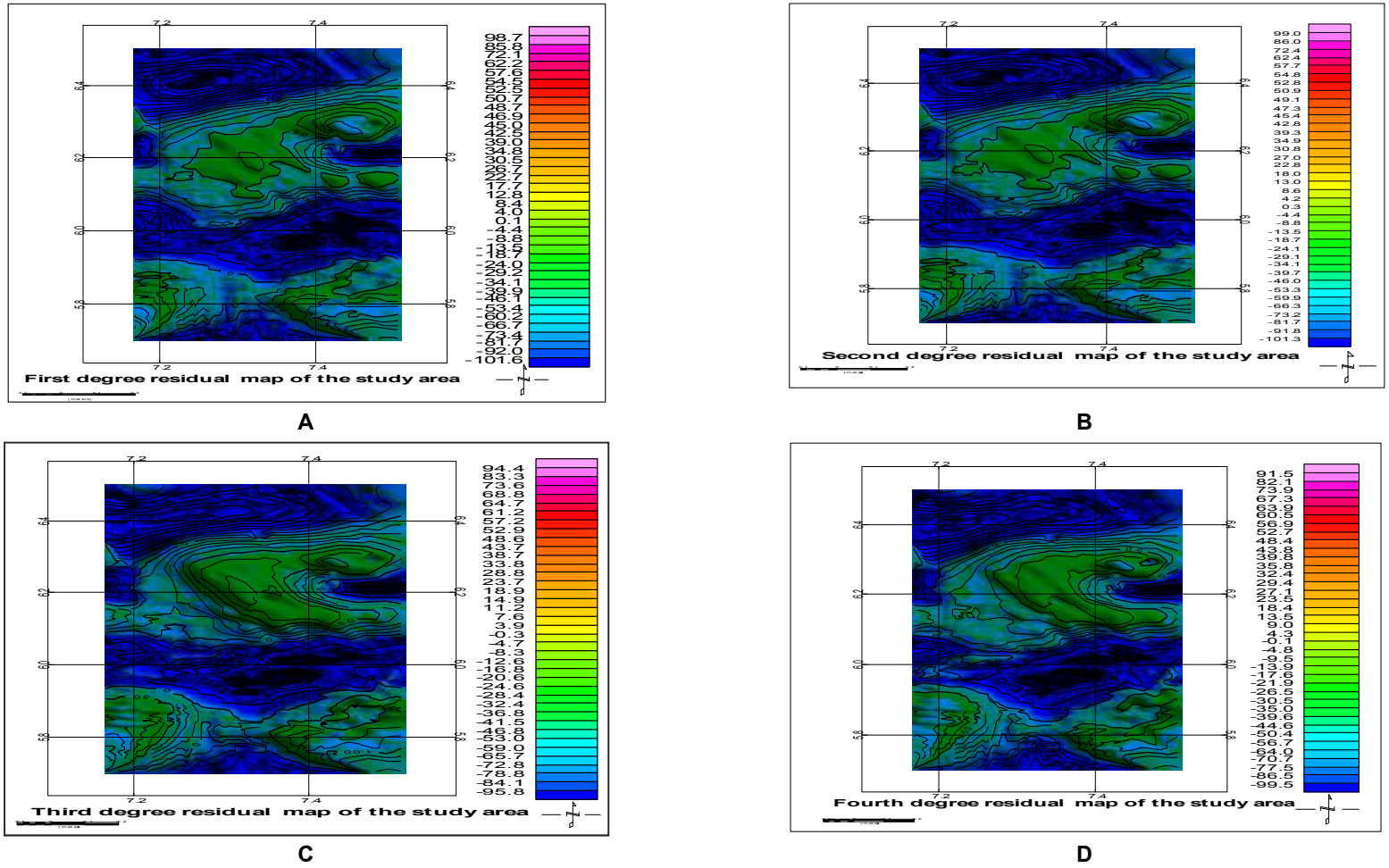

Fig. 5. First to fourth degree residual fields of the aeromagnetic data: (a) First degree (b) Second degree (c) Third degree (d) Fourth degree

Table 2. Calculated depth to magnetic source of the aeromagnetic map of study area

Town	Anomaly	Coordinates		Depth estimation in KM			Width (KM)	Amplitude in Gamma	Magnetization (A/M)	1% Radiance	Type of anomaly
Okigwe		Lat	Long	Peter's slope	Tiburg	Half width					
	A	5.4837	7.4375	0.598	1.121	0.748	5	7755	0.34	1.45	Low
	B	5.7675	7.3727	0.9105	1.724	1.248	5.5	7735	0.48	1.40	Low
	C	5.8763	7.4720	0.598	1.59	1.148	4.0	7850	2.34	1.47	Low
	D	5.4494	7.4657	0.723	1.8245	1.298	4.7	7754	1.42	1.42	Low
	E	5.6510	7.4287	1.223	1.624	1.148	4.9	7931	2.45	1.57	High
Udi											
	A	6.4106	7.2545	3.285	4.941	3.648	8.5	7775	0.61	1.23	Low
	B	6.2075	7.4967	2.285	5.342	3.948	7.0	7960	4.04	1.31	High
	C	6.2129	7.4693	0.7855	1.858	1.348	8.0	7780	0.52	1.19	Low
	D	6.4578	7.4241	1.348	3.667	2.698	7.0	7849	1.21	1.17	Low
	E	6.1371	7.3023	0.410	1,18	0.848	5.5	7950	2.44	1.32	High
	F	6.1453	7.4187	1.1605	2.348	1.848	7.0	7931	2.11	1.35	High

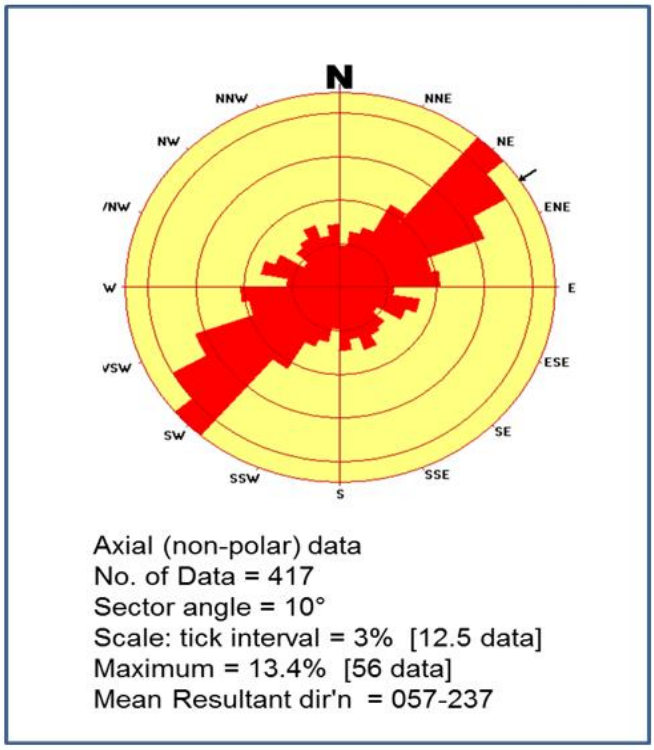

Fig. 6. Rose diagram of the study area

Results of the depth estimates to anomalous magnetic bodies using slope methods, 2-D spectral inversion and 3-D Standard Euler Deconvolution methods revealed depths ranging from 0.410 km to 4.94 km.The depth range to the various anomalous magnetic bodies estimated from the slope methods ranges from 0.598 to 1.724 km, within the Okigwe area (Fig. 8a) and 0.7855 to 4.941 km within the Udi area (Fig. 8b). The depth estimates using the Peter's slope, Tiburg and Half width slope methods are presented in Table 2.

Similarly, the power spectrum plots of the residual field of the study area revealed a two layer depth model (D_1 and D_2). The first layer depth (represented by the second segment of the spectrum D_1), is interpreted as the depth to the shallower anomalous magnetic sources (Figs. 9a and 9b). This layer (D_1) varies from 0.223 km to 1.048 km, with an average of 0.641 km. The second layer depth (D_2) varies from 2.459 km to 3.748 km, with an average of 3.088 km. This layer is believed to be as the result of magnetic basement rock, lateral variations in basement susceptibilities, and possibly intra-basement features like faults and fractures probably resulting from tectonism [35]. It can be deduced that the D_2 values obtained from the spectral plots represent the average depths to the basement complex in the area under study.

The depth to the shallower magnetic sources increases from the northeastern part of the study area to the southern part (Fig. 10) while the magnetic basement depth increases from the northwestern part of the study area to the southern part (Fig. 11). It can be deduced that the basement is shallowest within the western part of Enugu. Similarly, the southern part of the study area is believed to have much thicker sediment pile because the basement is deeper in those areas. Such areas hold much prospect for generation of hydrocarbon deposits because of its thick sedimentary pile.

3-D standard Euler deconvolution of the aeromagnetic data of the study area using different structural indices revealed standard Euler solution clusters as shown in the maps (Figs.12a – 12d). In order to differentiate between the various solutions, unwanted solutions which interfere with proper understanding of the obtained solutions must be removed. Therefore, the elimination of these unwanted solutions determines the choice of

depth range used in differentiating the solutions. The interpreted depth ranges for this study ranges from 0 to 3000 m which enhances a better comparison of the solutions obtained. A wide range of geologic models such as: contacts, dyke/sill, horizontal cylinder/pipes and spheres, with structural indices of 0 to 3 were used to derive the 3-D Standard Euler solutions. For this study, the solutions for four geological models with magnetic structural indices of 0-3 are presented. Result for magnetic contacts (structural index=0) is shown in Fig. 12a. Fig. 12a revealed an Euler depth range between 250m to above 3000m, with heavily concentrated clusters of solutions seen around Lekwesi, Lokpanta, Lokpaukwu and Isuochi areas. Other places where slightly concentrated clusters of solutions exist are Awgu, Ngwo, Enugu and Agbani areas. This indicates that magnetic contact is a major geological feature dominating a major part of the study area. Similarly 3-D Standard Euler solutions indicating sills/dykes geological models are presented for structural index of 1 (Fig. 12b). The depth estimates of this model in the study area revealed a range of 500m to a little above 3000 m. Fig. 12b shows that sills/dykes are dominant around Lekwesi, Lokpanta, Lokpaukwu and Isuochi areas with clusters of solutions found within those areas. Other areas where clusters of solutions are seen are within Awgu and the western part of Enugu. There is however a near absence of clusters in the southern portion of the study area. Similarly, for horizontal cylinders/ pipes as represented by structural index of 2 (Fig.12c), the depth estimate within the study area is between 1000m and a little above 3000 m; With isolated clusters of solution within the areas. Fig. 12d shows heavy build up of cluster solutions for the sphere models with structural index (S.I =3). The depth estimates for this model ranges from 500m to about 3000 m (Fig.12d). Fig. 12d revealed that the spheres are more prominent within Awgu, and along Lokpanta –Lokpaukwu -Lekwesi axis. Unlike the contacts, spheres are sparsely distributed within the study area. The results of depth to anomalous basement from these three methods revealed a high level of agreement. The average basement depth value of 3.088 km interpreted for the study area is in line with results of earlier studies carried out within the study area [6,9,36,37].

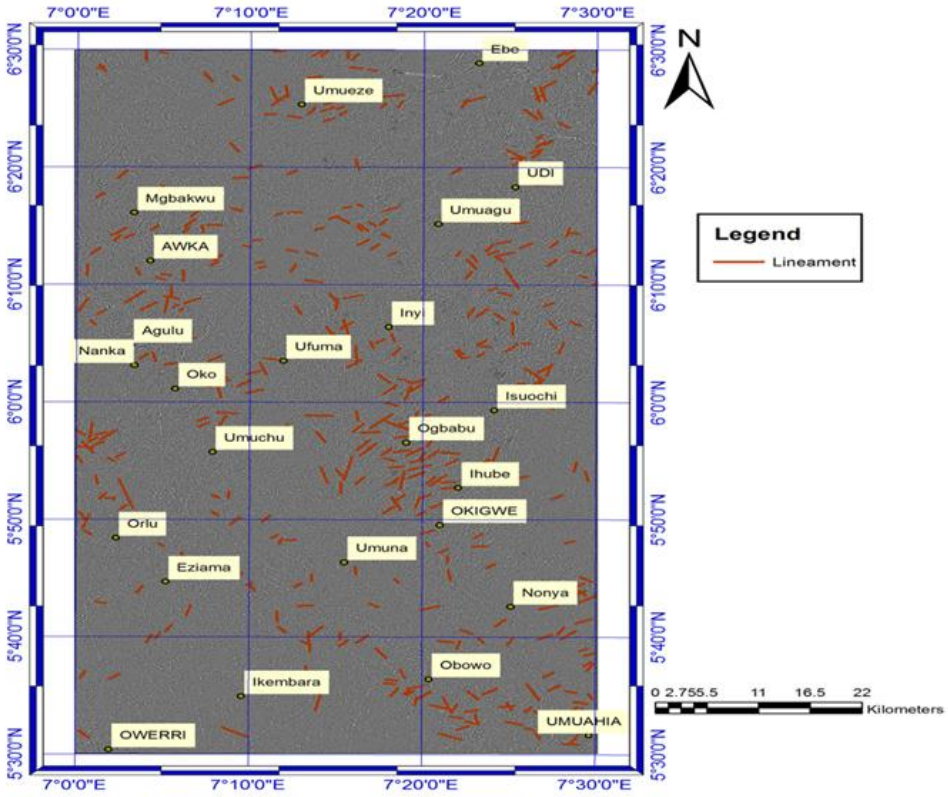

Fig. 7. Lineament draped on edge-enhanced map of the study area

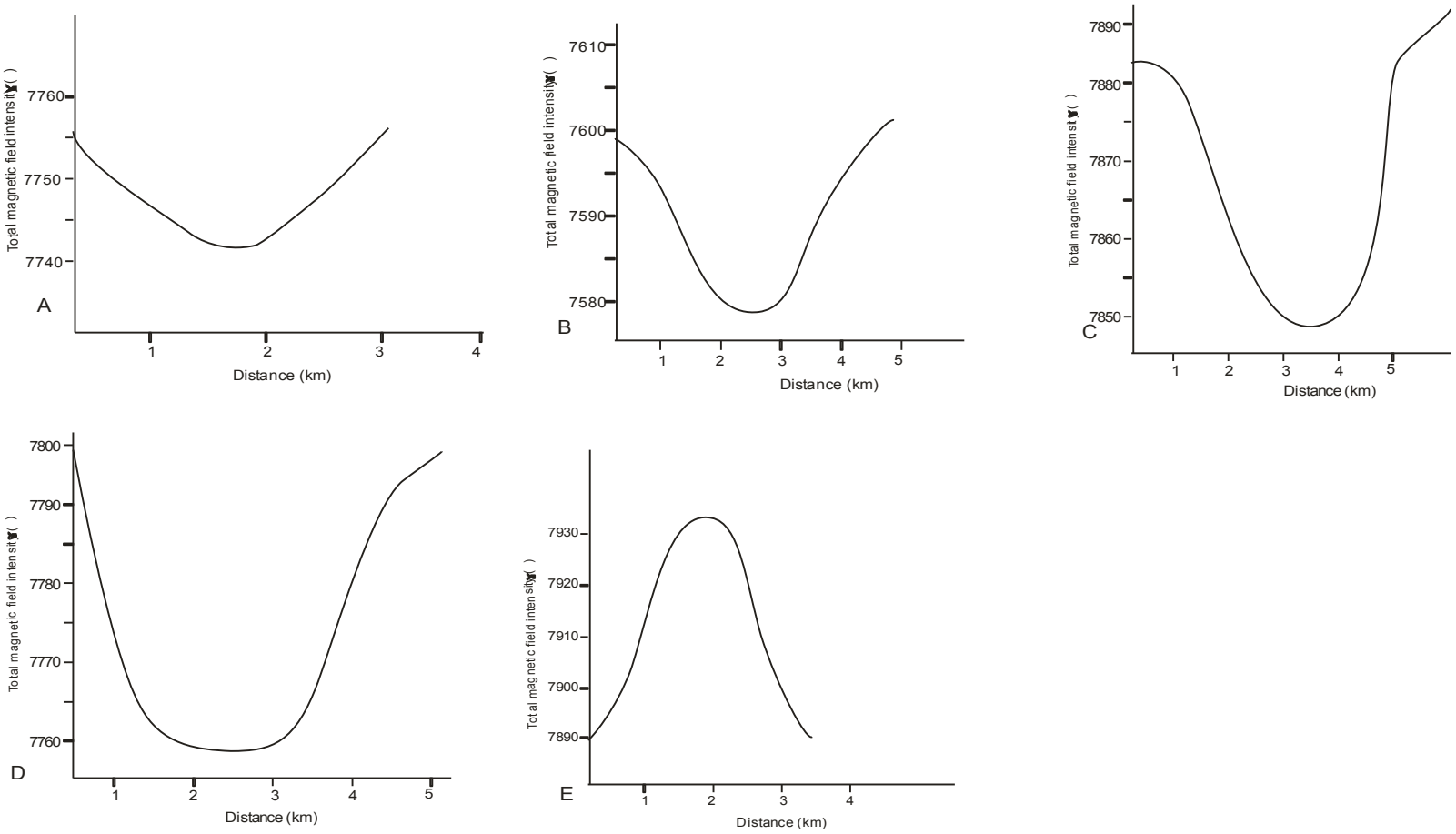

Fig. 8a. Interpretation of some linear magnetic anomalies from Okigwe Sheet. Profiles A-E are taken as follows: Profile (A), 30 km S.E of Okigwe; Profile (B), Okigwe; Profile (C),1 km SW of Okigwe; Profile (D), 1 km N.E of Okigwe; Profile E, 2 km South-west of Okigwe

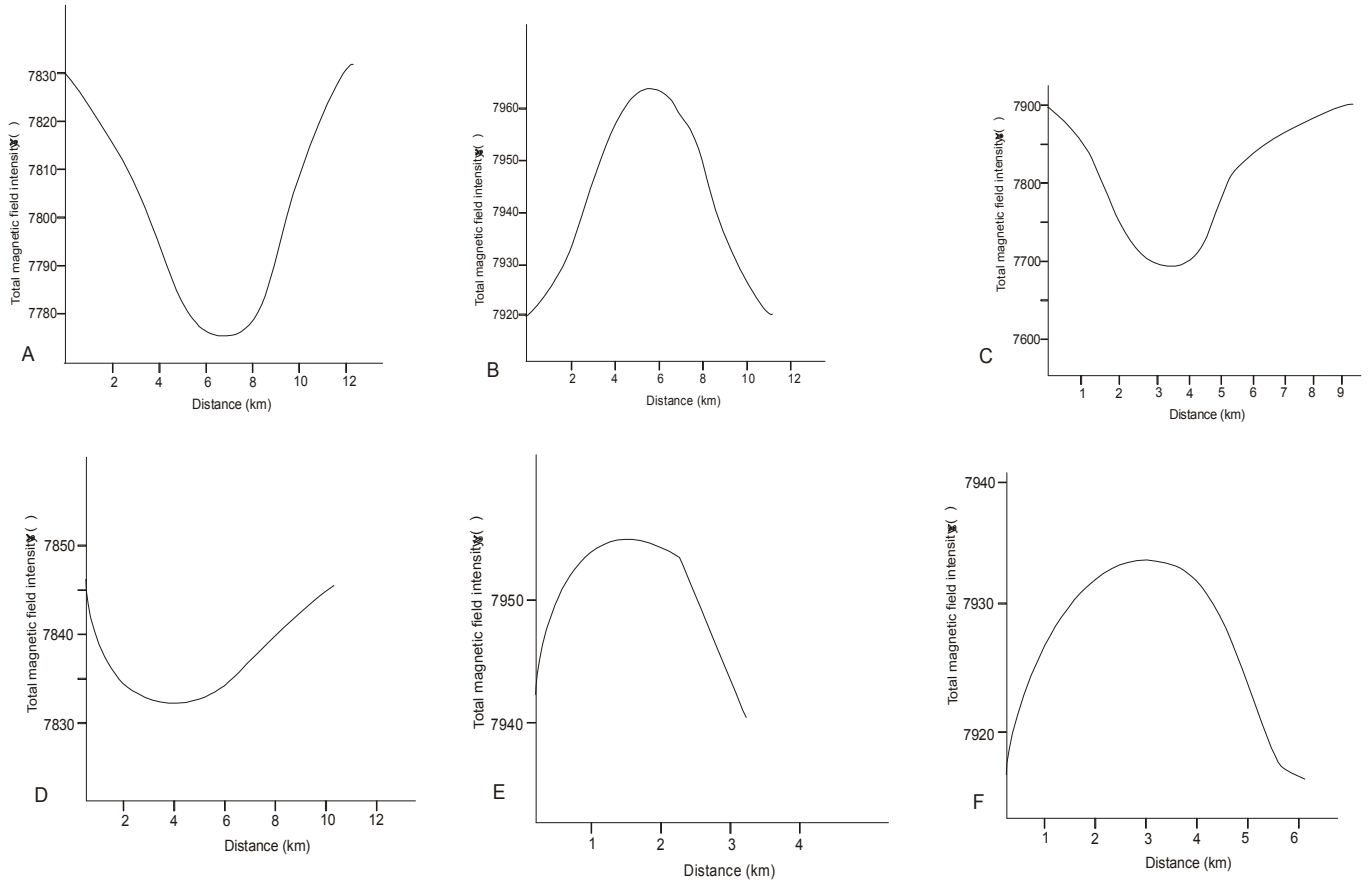

Fig. 8b. Interpretation of some linear magnetic anomalies from Udi sheet. Profiles A-F were taken as follows; Profile (A), 9 km south-east of Amadim; Profile (B), Udi town; Profile (C), 12 km south-east of Udi; Profile (D), 7.6 km west of Enugu; Profile (E), 4 km North-West of Obu-Inyi; Profile (F), 10 km of North-West of Awgu

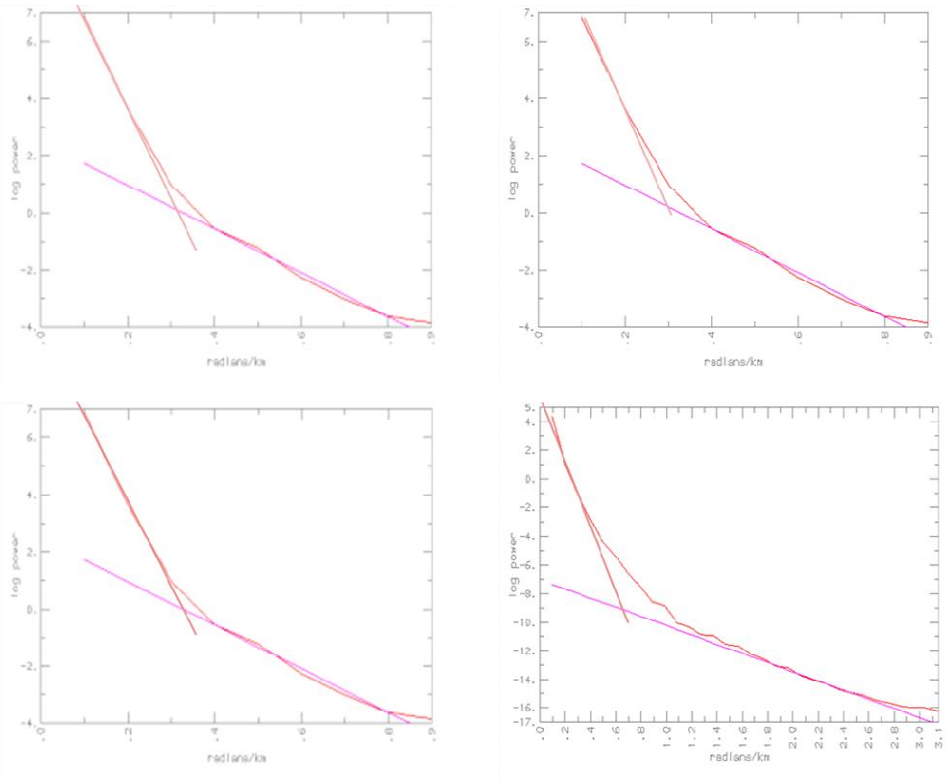

Fig. 9a. Spectral plots of aeromagnetic data of Okigwe sheet

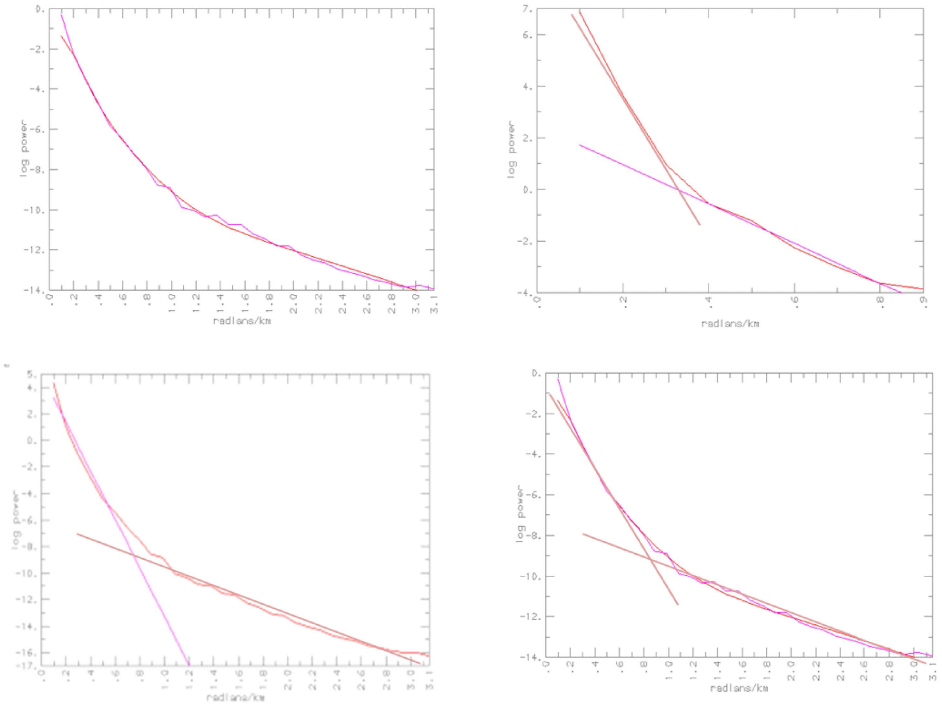

Fig. 9b. Spectral plots of aeromagnetic data of Udi sheet

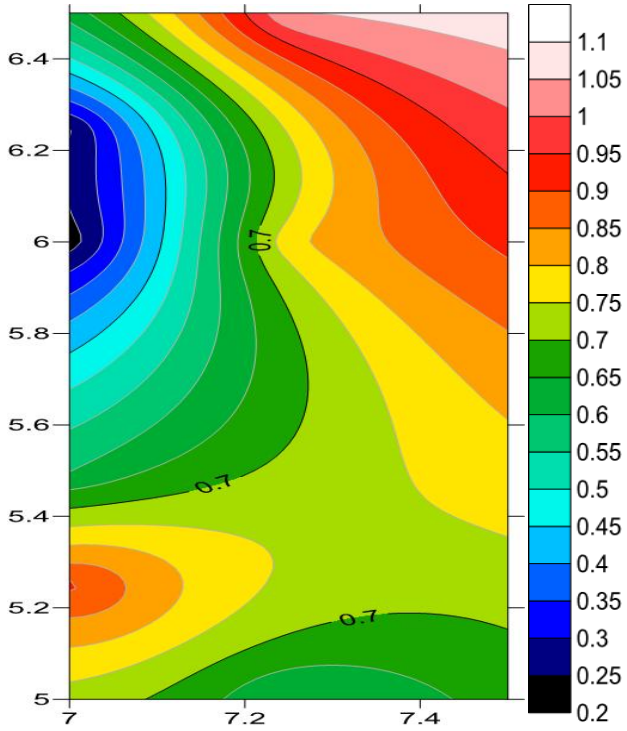

Fig. 10. Depth to shallower anomalies (D_1) map of the study area

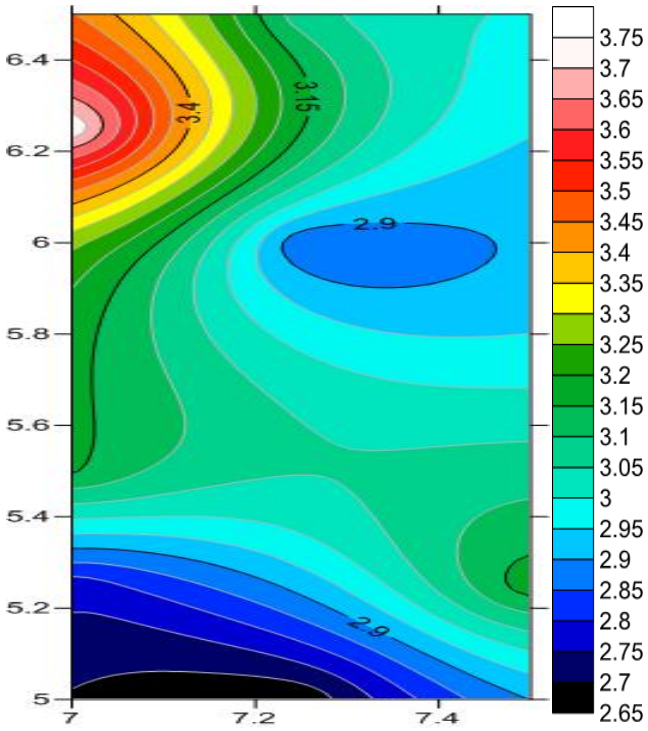

Fig. 11. Depth to deeper anomalies (D_2) map of the study area

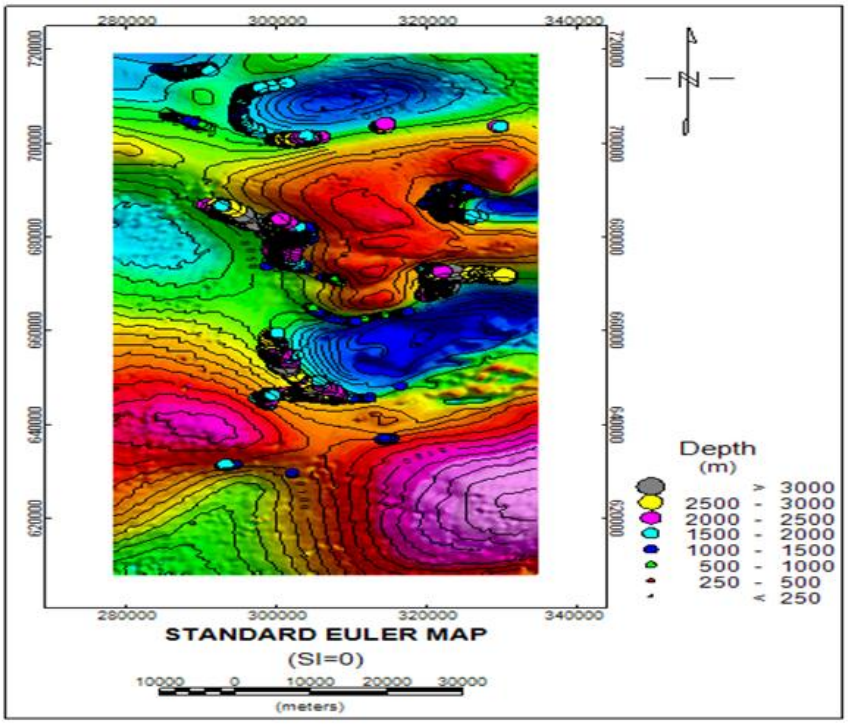

Fig. 12a. Standard Euler deconvolution depth solution plot draped on the colour shaded grid of the total magnetic intensity of the study area (Structural index=0)

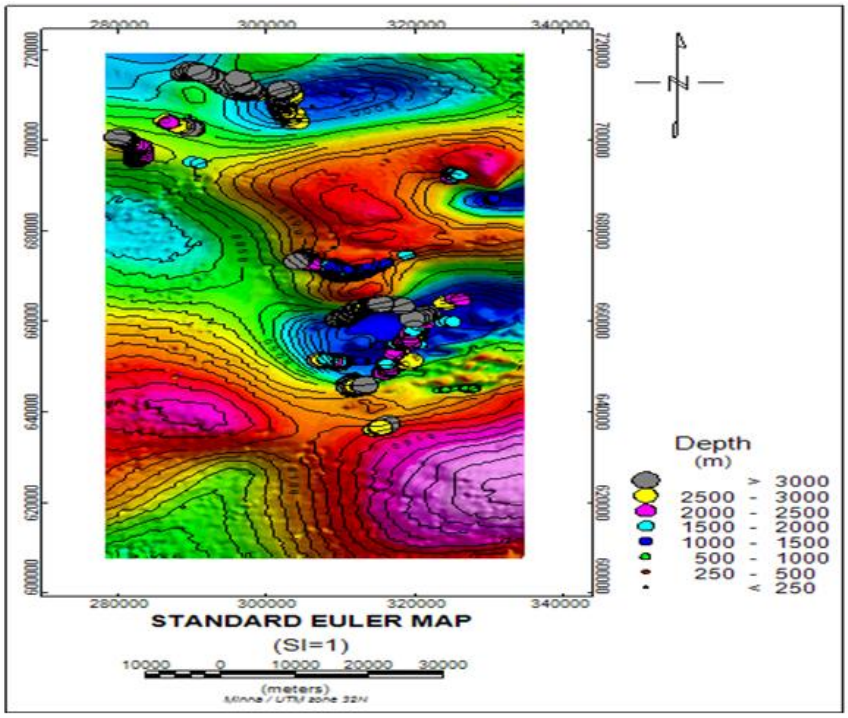

Fig. 12b. Standard Euler deconvolution depth solution plot draped on the colour shaded grid of the total magnetic intensity of the study area (Structural index=1)

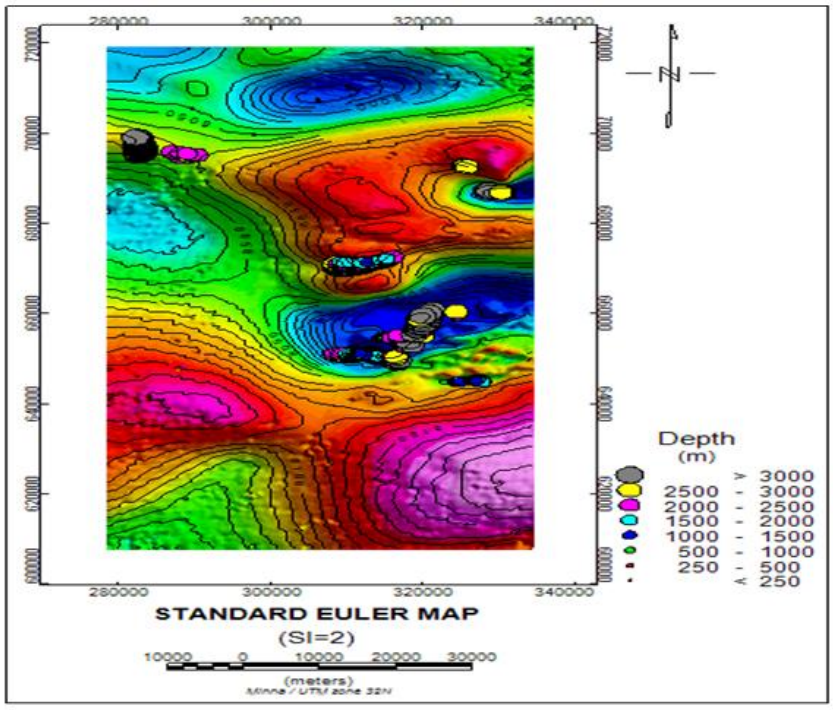

Fig. 12c. Standard Euler deconvolution depth solution plot draped on the colour shaded grid of the total magnetic intensity of the study area (Structural Index=2)

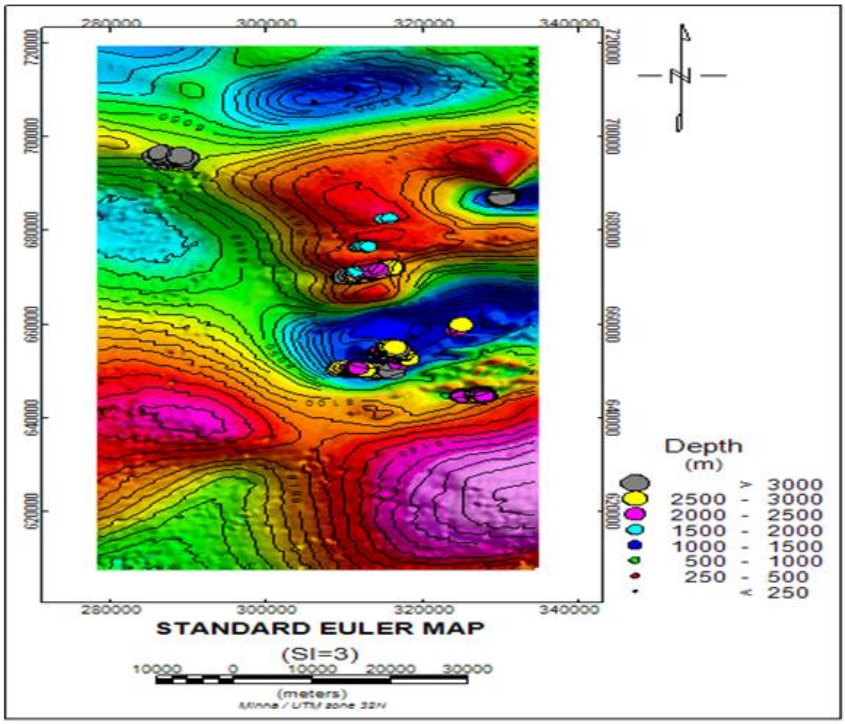

Fig. 12d. Standard Euler deconvolution depth solution plot draped on the colour shaded grid of the total magnetic intensity of the study area (Structural index=3)

4. CONCLUSION

Several linear and tectonic features have been interpreted from the study area with lineaments with structural trends of NE-SW direction been dominant. The study area have also been interpreted as a sedimentary basin with an average sedimentary thickness of approximately 3.088 km. The sedimentary thickness interpreted in the study area makes the area viable for hydrocarbon generation and accumulation. Sediment thickness greater than 2 km is normally favourable for thermal maturation of potential source rocks [22]. Similarly, several igneous intrusive bodies were interpreted from the study area and associated with high temperature regimes. The accompanying high temperature gradient associated with the intrusive igneous/metamorphic rocks may have over cooked the source rocks present beyond the oil window phase and may have result resulted to over maturation. The presence of these intrusive bodies may be potential sources of minerals and dioritic/igneous bodies that can be used as aggregates for construction.

Structural interpretation and assessment of depth to anomalous basement was carried out using slope (graphical) methods, standard 3-D Euler deconvolution and 2-D spectral inversion techniques. The presence of pipes within the study area infers the points of intersection between geological faults. Similarly, the presence of intrusive bodies in part of the study area suggests that some area is more tectonically active than some others. Such areas like Okigwe, Orodo and Orlu are tectonically quiet owing to the absence of deep-seated anomalies and intrusive bodies. Structural analysis using 3-D Standard Euler deconvolution with structural indices ranging from 0-3 revealed the dominant presence of three geological models which include spheres, horizontal pipes/cylinders and sills/ dikes. 2-D spectral analysis of the study area revealed a two layer depth model. The first layer (D_1) depth varies from 0.223 to 1.048 km, with an average of 0.641 km. The second layer depth (D_2), obtained from the spectral plots represent the average depths to the basement complex in the blocks considered. It varies from 2.659 km to 3.748 km, with an average of 3.088 km. This layer may be attributed to magnetic rocks of the basement surface, lateral variations in basement susceptibilities, and intra-basement features like faults and fractures [35]. Depth to source interpretation of aeromagnetic field data provided important information on basin architecture for both petroleum and mineral exploration mapping for areas with shallow basement. Finally, magnetic depth from the standard 3-D Euler deconvolution revealed a depth of 0 to above 3000m, which is very similar to those obtained elsewhere in the Benue trough. [36] estimated depth of 3.7 km within the Nkalagu area. [9] Deduced a depth of 2.289 km for the neighbouring Ugep area. The obtained depth is closely in agreement with the estimate of 3.3 km of the total thickness of the Cretaceous sediments in Nigeria as speculated [37]. The main magnetic structural trend of NE-SW direction which controls the basin orientation is suspected to be a continental extension of the oceanic Chain and Charcot fracture systems [12,33,34]. This trend represents significantly features of the tectonic and structural framework of the Anambra Basin.

The high magnetic intensity observed around Enugu, Udi and Okigwe suggests the existence of a deep-seated basement feature. The presence of the deep-seated structures in the study area confirms that the study area has been subjected to both regional stress and strain fields. Similarly, the presence of folded basement and pipes suggest that different stress-strain regimes operated within the study area in the past. This is evident by the faults and fold axes of the anticlinal fold interpreted within the study area, which has dominant NE-SW trend. Therefore, the basement topography of the study area reflects the effect of the past tectonic events which prevailed in the area. Hence, landform features including the Okigwe-Udi escarpment have direct bearing with the magnetic basement topography.

COMPETING INTERESTS

Authors have declared that no competing interests exist.

REFERENCES

1. Gunn PJ. Application of aeromagnetic surveys to sedimentary basin studies. AGSO Journal of Australian Geology and Geophysics. 1997;17(2):133-144.
2. Onyedim GC, Awoyemi EA. Aeromagnetic imaging of the basement morphology in the part of the middle benue trough. Journal of Mining and Geology. 2006; 42(2),157-163.

3. O'Leary DW, Friedman JD, Phn HA. Lineament, linear, lineation: Some proposed new standard for old terms. Geol. Soc. Amer. Bull. 1976;87:1463-1469.
4. Spector A. Grant FS. Statistical models for interpreting aeromagnetic data. Geophysics. 1970;35:293-302.
5. Opara AI. Estimation of the depth to magnetic basement in part of the dahomey basin, Southwestern Nigeria. Australian Journal of Basic and Applied Sciences. 2011;5(9):335-343.
6. Ofoegbu CO, Onuoha KM. Analysis of magnetic data over the abakaliki anticlinorium of the lower benue trough, Nigeria. Marine and Petr. Geol. 1991;8.
7. Udensi EE, Osazuwa IB. Spectral determination of depths to buried magnetic rocks under the nupe basin, Nigeria. Proceedings of the 23rd annual conference of the Nigerian Institute of Physics. The Millenium Conference. 2000;170-176.
8. Udensi EE, Osazuwa IB. Spectral determination of depth to buried magnetic rocks under the nupe basin, Nigeria. Nigerian Association of Petroleum Explorationists Bulletin. 2004;17(1):22-27.
9. Opara AI, Onyewuchi RA, Selemo AOI, Onyekuru SO, Ubechu BO, Emberga TT, Ibim DF, Nosiri OP. Structural and tectonic features of ugep and environs, calabar flank, Southeastern Nigeria: Evidences from Airborne Magnetic and Landsat- ETM data. Mitteilungen Klosterneuburg Journal. 2014;64.
10. Liu X. On the use of different methods for estimating magnetic depth. The Leading Edge. 2003;22:1090–1099.
11. Reijers TJ, Petters SW, Nwajide, CS. The Niger Delta Basin, in Selley RC, ed. African Basins--Sedimentary basin of the world 3: Amsterdam Elsevier Science. 1997;151-172.
12. Burke KG, Dessauvagie TFJ, Whiteman AJ. Geological history of the Benue Valley and adjacent areas. In: African Geology (Eds, Burke KG, Whiteman AJ), Geology Dept., Univ. of Ibadan, Nigeria. 1972;188-205.
13. Nwachukwu SO. The tectonic evolution of the Southern portion of the benue trough, Nigeria Geol. Mag. 1972;109:411-419.
14. Obi GC, Okogbue CO, Nwajide CS. Evolution of the Enugu Cuesta: A tectonically driven erosional process. Global Journal Pure Applied Sciences. 2001;7(2):321-330.
15. Murat RC. Stratigraphy and palaeography of the cretaceous and lower tertiary in Southern Nigeria. In: Dessauvagie TFJ, Whiteman AJ. (Eds.), African Geology, University of Ibadan, Nigeria. 1972;251-266.
16. Benkhelil J. Structure et evolution geodynamique du Basin intracontinental de la Benoue (Nigeria) Bull. Centres Rech., Explor. Prod. Elf Aquitaine. 1988;1207:29-128.
17. Okereke CS, Edet AE. Delineation of shallow groundwater aquifers in the coastal plain sands of the Calabar area (Southern Nigeria) using surface resistivity and hydrogeological data. Journal of African Earth Sciences. 2002;35:433–443.
18. Edet AE. Hydrogeology of parts of Cross River State, Nigeria: Evidence from aerogeological and surface resistivity studies. PhD Dissertation, University of Calabar, Calabar, Nigeria. 1993;316.
19. Obi CG. Depositional model for the Campanian-Maastrichtian succession, Anambra basin, Southeastern Nigeria. Unpublished Ph.D Thesis University of Nigeria, Nsukka. 2000;291.
20. Oboh-Ikuenobe FE, Obi CG, Jaramillo CA. Lithofacies, palynofacies, and sequence stratigraphy of Palaeogene strata in Southeastern Nigeria. Journ. of Afr. Earth Sci. 2005;41:79-101.
21. Akpabio I, Ekpo E. Geo-electric investigation for groundwater development of Southern part of Nigeria. Pacific Journal of Science and Technology. 2008; 9(1):219–226.
22. Wright JB. Geology and mineral resources of West Africa. George Allen & Unwin, London. 1985;187.
23. Reyment RA. Aspects of geology of Nigeria, Ibadan University Press, Ibadan Nigeria. 1965;106.
24. Olade MA. Evolution of Nigeria's benue trough (aulacogen): A tectonic model. Geol. Mag. 1975;112:576-583.
25. Ozoko DC. Origin of dissolved solids in Cretacous Aquifers at Ngbo, Ebonyi State, Nigeria. A Preliminary Assessment. Int. Journal of Innovative Science, Engr. and Technology. 2015;2(6):247-253.
26. Thompson DT. EULDPH: A new technique for making computer-assisted depth estimates from magnetic data. Geophysics. 1982;47:31-37.

27. Reid AB, Allsop JM, Granser H, Millett AJ, Somerton IW. Magnetic interpretation in three dimensions using euler deconvolution. Geophysics. 1990;55: 80-91.
28. Hood P. Gradient measurements in aeromagnetic surveying. Geophysics. 1965;30:891-902.
29. Whitehead N, Musselman C. Montaj gravity/magnetic interpretation: Processing, analysis and visualization system for 3-d inversion of potential field data for oasis montaj v6.3, Geosoft Incorporated, 85 Richmond St. W., Toronto, Ontario, M5H 2C9, Canada; 2008.
30. Gay SP. Fundamental characteristics of aeromagnetic lineaments: Their geological significance and tectonic significance to geology, Salt Lake city, Utah. American Stereo Map. 1972;94.
31. Ghazala HH. Geological and structural interpretation of airborne surveys and its significance for mineralization, South Eastern Desert, Egypt. Jour. Of African Earth Sciences. 1993;16(3):273-285.
32. Zaborski PM. A review of the cretaceous system in Nigeria. African Geoscience Review. 1998;5(4):385-400.
33. Ananaba SE. Dam sites and crustal megalineaments in Nigeria. ITC Journal. 1991;1:26-29.
34. Okereke CN, Ananaba SE. Deep crustal lineament inferred from aeromagnetic anomalies over the Niger Delta, Nigeria. Journ. of Mining and Geol. 2006;42(2):127-131.
35. Kangoko R, Ojo SB, Umego MN. Estimation of basement depths in the Middle Cross River basin by Spectral analysis of the Aeromagnetic field. Nig. Journ. of Phys. 1997;9:30-36.
36. Onyewuchi RA, Opara AI, Ahiarakwem CA, Oko FU. Geological interpretation inferred from airborne magnetic and landsat data: Case Study of Nkalagu Southeastern Nigeria. International Journ. of Science and Technology. 2012;2(4): 178-191.
37. Kogbe CA. The cretaceous and paleogene sediments of Southern Nigeria. Geology of Nigeria 2nd Edition. Rock View (Nig) Ltd. 1989;325-334.

Peer-review history:
The peer review history for this paper can be accessed here:
http://sciencedomain.org/review-history/18815